Journal of Atomic, Molecular, Condensate & Nano Physics
Vol. 2, No. 2, pp. 73–84, 2015
ISSN 2349-2716 (online); 2349-6088 (print)
Published by RGN Publications

http://www.rgnpublications.com

Effect of Debye Plasma on Hydrogenic Photoionization Cross Section

Research Article

Madhusmita Das* and N. K. Gupta

Theoretical Physics Division, Bhabha Atomic Research Center, Mumbai 400085, India
***Corresponding author:** msdas@barc.gov.in

Abstract. In this work, we have studied the effect of plasma screening on the ground and excited state photoionization cross section (σ) of hydrogenic system. We have considered weakly coupled plasma where the screening of nuclear charge by plasma free electrons is represented by Debye-Huckel potential. Using this potential, radial Schrodinger equation is solved numerically to obtain the bound and free state wave functions, and transition matrix elements. Adaptive step size controlled Runge-Kutta method is used for numerical integration. Use of adaptive method for grid generation ensures lesser computational time as compared to uniform grid system. Using the methodology, we have computed photoionization cross section from $1s$ ground state and excited $2p$ state of hydrogenic system. Strong enhancements in σ are observed which are generally termed as shape resonances. It is noted that these resonances occur for specific screening values where bound states are pressure ionized to enter the quasi-bound regime. The changes in the phase and amplitude of continuum wave functions also lead to appearance of Cooper minimum in σ of excited $2s$ state. We have compared the results with existing theoretical and experimental data wherever they are available.

Keywords. Debye-Huckel potential; Pressure ionization; Shape resonance; Cooper minimum

PACS. 50.

Received: April 6, 2015 **Accepted:** September 22, 2015

1. Introduction

Photoionization [1,2] is one of the significant modes of energy absorption process in radiation-matter interaction. It has important applications in many fields of physics such as laser produced plasma, *inertial confinement fusion* (ICF), astrophysical systems, x-ray lasers, plasma spectroscopy, etc. In all these systems, matter exists in plasma form and ions present in it are subjected to additional charge distribution created by neighboring ions and electrons. The electronic properties of ions in such an environment are thus highly altered and give rise to many interesting features in the photoionization [1,2] cross section. Study of photoionization cross section of isolated atomic system is a field pursued over for many decades. However, in recent days, considerable effort is being put in to understand the plasma effect on the cross section. The presence of external charge distribution in plasma alters the atomic potential experienced by the electrons. As a result the energy levels and wave functions (bound and continuum) get modified to great extent. Continuum lowering [5–10] and pressure ionization [6,11–15] are two important manifestation of plasma environment on the bound levels. The modified potential around the ion due to plasma free electrons gives positive shift to its energy levels. As a result the ionization potential for that level is lowered leading to continuum lowering. Apart from this, the presence of neighbouring ions gives rise to phenomenon of pressure ionization. This is an important artifact of nuclear charge screening on bound levels. This phenomenon arises due to overlap of wave functions of outermost levels of neighbouring ions which results in formation of band. In this regime bound levels are pressure ionized and electrons are treated as free. Because of pressure ionization, there exists finite number of bound levels in ions which are subjected to plasma environment. Pressure ionization of bound levels and modifications in bound and continuum state wave functions lead to remarkable changes in photoionization cross section.

Though plasma free electrons and ions are responsible for the modification in the atomic potential, there exists no analytical expressions to account for the effects. Depending on the plasma conditions i.e. density and temperature, model potentials are available to account for the effect of the plasma free electrons on the bound electrons via nuclear charge screening. Most popular model potentials [3,4] are Debye-Huckel (DH) potential and ion sphere (IS) potential. The choice of particular form depends on the plasma coupling parameter $\Gamma = \frac{E_{\text{Coulomb}}}{E_{\text{thermal}}} = \frac{Q^2}{4\pi\epsilon_0 a \kappa_B T}$, where Q is the charge on the particles, $a = \left(\frac{3}{4}\pi n\right)^{\frac{1}{3}}$ is the inter particle separation, n denotes plasma number density and T is the temperature of plasma. In case of low dense and high temperature plasma, thermal energy dominates over the Coulomb interaction. Such kind of plasma is categorized as weakly coupled one for which $\Gamma < 1$. Typical density and temperature ranges appearing in such kind of plasma are $n_{\text{ion}} \sim 10^{15} - 10^{18}\ \text{cm}^{-3}$, $T \sim 0.5 - 5$ eV (stellar atmosphere), $n_{\text{ion}} \sim 10^{19} - 10^{21}\ \text{cm}^{-3}$, $T \sim 50 - 200$ eV (laser produced plasma) etc. DH potential is the most widely used potential to obtain the electronic properties of ions in this kind of plasma. DH model approximates the average interaction of ion with plasma particles where the plasma is considered to be a classical one with degeneracy parameter $\gamma \sim \frac{n^{2/3}}{T_e} \ll 1$. Due to weak interactions, the equations describing the potentials can be linearized leading to simple form ($\propto e^{-\mu r}$) for screening effect, μ represents the screening strength [4].

Computation of photoionization cross section of ions embeded in Debye plasma requires knowledge of spectral properties such as ionization potential, bound-free transition matrix element etc. These data can be generated by solving the radial Schrodinger equation using DH potential. There exists various techniques like Ritz variation method, sympletic integration scheme, basis set expansion method, complex co-ordinate rotation method, constrained interpolation polynomial method (CIP) etc., which can be used to compute photoionization cross section. Jung et al. [16], have used Ritz variation method to investigate the effect of dense plasma on photoionization cross section. Qi et al. [17] have used sympletic integration scheme to study photoionization dynamics in hydrogen like systems. Their study reveals the presence of resonance structures in photoionization cross section. Simillar feature in the hydrogenic photoionization cross section is also observed by Lin et al. [18] using complex co-ordinate rotation method.

In this article, we discuss the effect of Debye plasma on ground and excited state photoionization cross section of hydrogen like system using CIP method [19]. In this methodology, the radial Schrodinger equation is solved numerically using shooting method approach, where adaptive step size controlled Runge-Kutta method is employed to do the integration. The computed bound and continuum state wave functions are used to calculate the photoionization cross section in non relativistic dipole approximation. The main findings of this investigation are occurrence of shape resonance and Cooper minimum. The paper is structured as follows. In Section 2, the computational methodology is discussed. Results and important findings are discussed Section in 3. Finally, conclusion is given in Section 4.

2. Theory and Computational Method

The atomic photoionization cross section for $nl \to \epsilon l'$ transition in non relativistic dipole approximation ($l' - l = \pm 1$) is given by [20,21]

$$\sigma_{nl} = \frac{8\pi^2 \alpha a_0^2}{3(2l+1)}\left(\epsilon + I_{nl}\right)\left[l\, {R_{nl}^{\epsilon l-1}}^2 + (l+1){R_{nl}^{\epsilon l+1}}^2\right] \tag{2.1}$$

where, a_0 and α represent Bohr radius and fine structure constant respectively. ϵ is the energy of photo electron ejected from the ion. I_{nl} is the binding energy of nl state. $h\nu = I_{nl} + \epsilon$ represents the energy of the incident photon causing the radiative transition. Here,

$$\begin{aligned} R_{nl}^{\epsilon l \pm 1} &= \langle P_{nl} | r | P_{\epsilon\, l\pm 1} \rangle \\ &= \int_0^\infty P_{nl}(r)\, r\, P_{\epsilon\, l\pm 1}(r) dr \end{aligned} \tag{2.2}$$

$P_{nl}(r)$ and $P_{\epsilon l}(r)$ represent the radial part of bound and continuum state wave functions which are obtained by solving the Schrodinger equation with appropriate potential $V(r)$. The equation can be written as follows [22]

$$\frac{d^2 P_{kl}(r)}{dr^2} + \left(2E_{kl} - 2V(r) - \frac{l(l+1)}{r^2}\right) P_{kl}(r) = 0. \tag{2.3}$$

Here $k = n$ (principal quantum number) for bound states ($E_{nl} < 0$) and $k = \sqrt{2\epsilon}$ for continuum state ($E_{kl} = \epsilon > 0$ is the continuum state energy). l represents angular momentum quantum number. $P_{kl}(r)$ is the radial part of the wave function represented as $\Psi_{klm}(r,\theta,\phi) = \frac{P_{kl}(r)}{r} Y_m^l(\theta,\phi)$.

In case of a weakly coupled Debye plasma, the potential $V(r)$ can be written as follows [3].

$$V(r) = -\frac{Z}{r}e^{-\mu r}. \tag{2.4}$$

Here, μ represents the screening strength which is related to electron number density n_e and temperature T through the relation $\mu = \sqrt{\frac{4\pi n_e e^2}{k_B T_e}}$. The presence of screening function in the potential makes the potential short range. This property of modified atomic potential has great many effects on photoionization cross section. In this potential, the boundary and normalization conditions satisfied by the bound wave functions $P_{nl}(r)$ are given as follows [19]:

$$P_{nl}(0) = 0 \; ; \; P_{nl}(r \to \infty) = 0$$
$$\int_0^\infty P_{nl}(r)^2 dr = 1 \tag{2.5}$$

Continuum state wave functions satisfy different normalization and boundary conditions. At origin, continuum state radial function $P_{\epsilon l}$ satisfies the same boundary condition as bound state functions but at $r \to \infty$, it exhibits asymptotic behaviour. The conditions are given as follows [19]:

$$P_{\epsilon l}(0) = 0$$
$$P_{\epsilon l}(r \to \infty) \sim \sqrt{\frac{2}{\pi k}} \sin\left(kr - l\frac{\pi}{2} + \delta_\epsilon\right)$$
$$\int_0^\infty P_{\epsilon l} P_{\epsilon' l} dr = \delta(\epsilon - \epsilon'). \tag{2.6}$$

Here, δ_ϵ represents the phase shift. Eq.(2.3) is solved for bound states ($E_{nl} < 0$) and continuum states ($\epsilon > 0$) using the numerical methodology developed by Utsumi *et al.* [19] with proper boundary and normalization conditions. The details of the method is given in Ref [19] and is not discussed here. In this approach, the second order boundary value problem is converted into coupled first order initial value problem and shooting method approach is used to solve the coupled linear equations using the numerical integration techniques based on adaptive step size controlled Runge-Kutta Method. Use of adaptive method for grid generation ensures lesser computational time as compared to uniform grid system. This method is a powerful tool to solve the free state wave functions. Here, highly oscillating continuum orbitals in far-field region are represented by Phase-Amplitude method ($P_{\epsilon l}(r) = y(r)\sin(\phi(r))$ where $y(r)$ and $\phi(r)$ respectively represent amplitude and phase of the wave function. The main advantage of this method is that at each grid point we can get the value of radial function as well as their respective first derivative ($Q_{nl} = dP_{nl}(r)/dr$ and $Q_{\epsilon l} = dP_{\epsilon l}(r)/dr$) which can be directly used for evaluation of radial integrals using *Constrained interpolation polynomial* (CIP) method as discussed in Ref. [19]. Using the knowledge of energies and wave functions (bound and free), one can evaluate all other transition properties of ions in plasma. For our calculation, we have set the relative accuracy of 10^{-8} for energy convergence.

3. Results and Discussion

Using the methodology as discussed in Section 2, we have computed excitation energies for various transitions in free hydrogenic system ($V(r) = -\frac{1}{r}$).The values are tabulated in Table 1. The accuracy of bound state energies are verified by comparing the excitation energies obtained from our calculation for $1s \to np$ and $2s \to np$ transitions with NIST data [23] as shown in Table 1. Table shows a reasonable agreement with the NIST data.

Table 1. Transition wavelength for H-atom in A^0

	Our result	NIST data [23]
$1s \to np$		
$n = 2$	1215.0531	1215.6701
3	1025.201	1025.728
4	972.0425	972.517
5	949.260	949.742
6	937.327	937.814
7	930.275	930.751
$2s \to np$		
$n = 2$	-	
3	6561.28	6562.77
4	4860.21	4861.29
5	4339.47	4340.47
6	4100.80	4101.73
7	3969.17	3970.07

We have investigated the effect of plasma screening on various electronic properties for $\mu \geq 0.001$ a.u. For very small values of screening strength i.e. very weakly coupled plasma, the electronic properties are not altered much. The system still behaves as free Hydrogenic system. However, with increase in μ, screening of nuclear charge by free electrons starts gaining prominence. Continuum lowering and pressure ionization are two important features which arise due to the nuclear charge screening by plasma free electrons. Figure 3 shows the decreasing behaviour of *ionization potential* (IP) of various $n\,l$ states of H atom. Screening of nuclear charge affects the higher excited states to large extent. Therefore, IP for these states decreases rapidly. However, the variation is slow for core states which are near the nucleus. With further increase in μ, the states become unbound resulting in finite number of bound states in ions. The gradual disappearance of bound levels leads to pressure ionization. The value of μ for which bound state merges into continuum is called critical screening strength μ_D^c. From Figure 3, it is observed that μ_D^c is smaller for high lying excited states and gradually increases for core states. The value of μ_D^c for various $n\,l$ states of hydrogen like system are given in Table 2. A comparison is also made with the data reported by Qi et al. [17]. A good agreement is observed between two sets of data. In Table 3, we have also compared the excitation energies for $1s \to np$ transition for different plasma conditions with that of Saha et al. [24] and good agreement is seen between two sets of data.

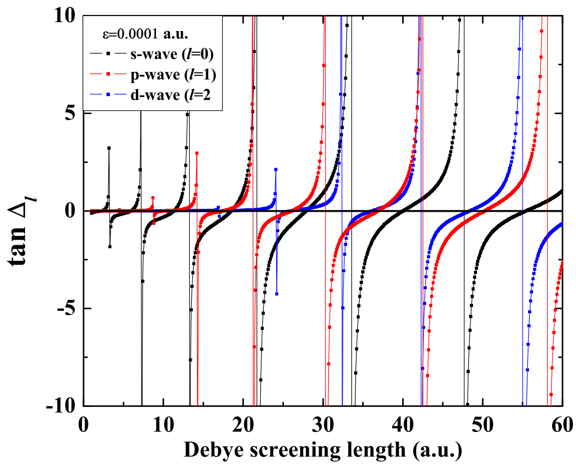

Figure 1. Variation of phases of continuum waves with Debye screening length at photoelectron energy $\epsilon = 0.0001$ a.u.

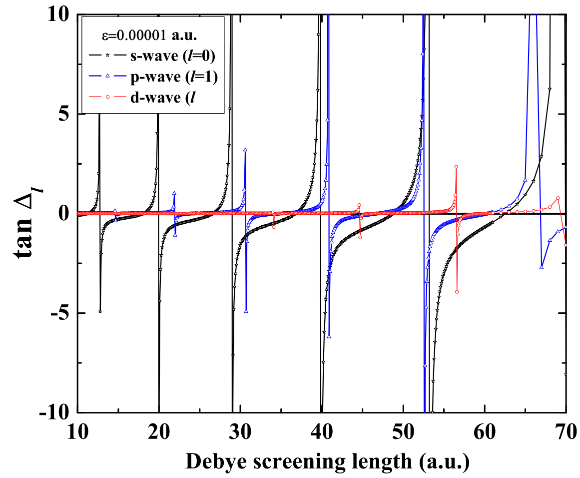

Figure 2. Variation of phases of continuum waves with Debye screening length at photoelectron energy $\epsilon = 0.00001$ a.u.

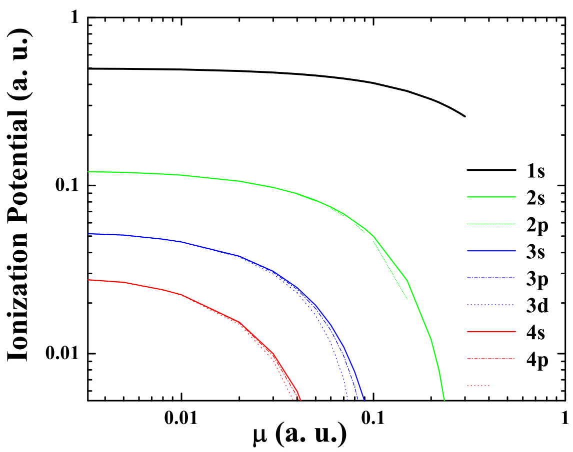

Figure 3. Variation of ionization potential for different levels of H atom with screening

Table 2. Critical screening strength μ_D^c for $n\,l$ states of H

$n \setminus l$	0	1	2	3	4	5
1	1.18966					
	(1.1906)[a]					
2	0.30966	0.22021				
	(0.310) [a]	(0.22021) [a]				
3	0.13906	0.11271	0.09134			
	(0.13943) [a]	(0.11271) [a]	(0.09134) [a]			
4	0.078519	0.06788	0.05810	0.04983		
	(0.07882) [a]	(0.06788) [a]	(0.05810) [a]	(0.04983) [a]		
5	0.05031	0.045182	0.04002	0.03538	0.03134	
	(0.05058) [a]	(0.045186) [a]	(0.04002) [a]	(0.03539) [a]	0.03134 [a]	
6	0.03493	0.03216	0.02916	0.02635	0.02379	0.02152
	(0.03517) [a]	(0.03217) [a]	(0.02916) [a]	(0.02635) [a]	(0.02379) [a]	(0.02152) [a]

[a] Qi et al. [17]

Table 3. Excitation energies for H-atom in Debye plasma

μ (a.u.)	Transition ($1s \to np$)	$E_{1s\to np}$(a.u.) (Our Result)	$E_{1s\to np}$(a.u.) (Saha *et al.* [24])
0.00	$1s \to 2p$	0.375	0.375
	$\to 3p$	0.44444	0.44444
	$\to 4p$	0.46874	0.46875
0.01	$\to 2p$	0.37483	0.37482
	$\to 3p$	0.44392	0.44392
	$\to 4p$	0.46776	0.46776
0.05	$\to 2p$	0.37108	0.37107
	$\to 3p$	0.43326	0.43325
0.08	$\to 2p$	0.36546	0.36545
	$\to 3p$	0.41824	0.41823
0.10	$\to 2p$	0.36052	0.36051
	$\to 3p$	0.40547	0.40546
0.20	$\to 2p$	0.32271	0.32263

Continuum state wave functions also exhibit very different behaviour with increasing μ. Due to screening, the phase and amplitude of continuum state are altered to great extent. The phase of continuum s, p and d waves are plotted in Figure 1 and 2 for $\epsilon = 0.0001$ a.u. and 0.00001 a.u., respectively. It is observed that the phase of these partial waves changes by π for specific values of screening strength. Careful investigation revealed that the phase change occurs for $\lambda_D^c = \frac{1}{\mu_D^c}$ where ns, np nd bound levels etc., are pressure ionized. It is also clear from the figure that the transition in phase becomes broader and broader as screening length is increased i.e. decreasing μ. Similar results are also reported by Qi *et al* [17].

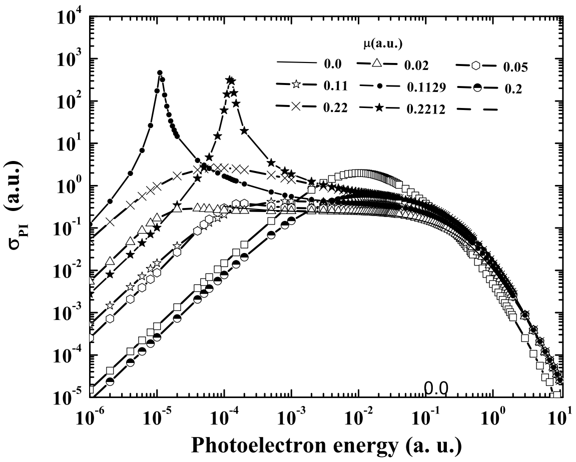

Figure 4. Variation of photoionization cross section from 1s state of Hydrogen atom with photoelectron energy for different μ.

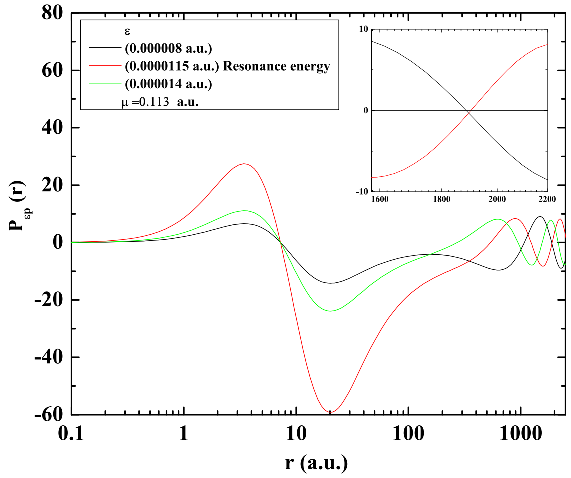

Figure 5. Continuum state wave functions for various energies near shape resonance arising due to 3p state. Inset shows the phase of wave resonance continuum state and state beyond resonance energy.

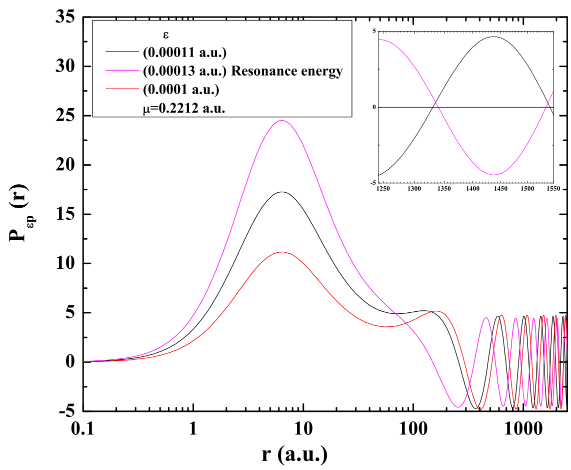

Figure 6. Continuum state wave functions for various energies near shape resonance arising due to 2p state. Inset shows the phase of wave resonance continuum state and state beyond resonance energy.

Using the bound and continuum wave functions we have computed the photoionization cross section of hydrogen atom for transition from ground $1s$ state and excited $2s$ state, As discussed in Sec. 2, photoionization cross section from nl state depends on the transition matrix elements $R_{nl}^{\epsilon l\pm 1}$ connecting transitions $n\,l \to \epsilon,\, l\pm 1$. For free hydrogenic system, where matrix elements can be expressed in closed form, it is a monotonic function of ϵ with finite threshold value. At higher energies, it satisfies asymptotic behaviour given as $\epsilon^{-7/2-l'}$, where l' is the continuum state angular momentum quantum number. However, in presence of plasma environment, it may behave very differently. The variation of $\sigma_{1s\to\epsilon p}$ with photo electron energy is given in Figure 4. Results are given for unscreened case ($\mu = 0$) and for various μ (0.02, 0.05, 0.11, 0.1129, 0.2, 0.22, 0.2212 a.u.). From the figure it is observed that for $\mu = 0$, the cross section has weak dependence on ϵ over a range and decreases afterwards. However, when screening is introduced in atomic potential, the cross section starts showing entirely different behaviour. The cross section shows very interesting features near the ionization threshold. In this low energy regime, cross section follows an increasing trend obeying Wigner-threshold law ($(2\epsilon)^{l'+1/2} = (2\epsilon)^{3/2}$) [25]. At higher photo electron energies, the behaviour is similar to that of unscreened case. As depicted in Figure 4, for specific values of μ, it shows large enhancements leading to resonance peaks. These peaks are commonly termed as ‘shape resonances’ as these are clear manifestation of the varying shape of the potential barrier i.e. $\frac{l(l+1)}{r^2}$ [26]. For hydrogen plasma, we have noticed shape resonance peaks at $\epsilon = 1.15\times 10^{-5}$ a.u. and 1.3×10^{-4} a.u. with respective μ values $\mu_r = 0.1129$ a.u. and $\mu_r = 0.2212$ a.u. These μ values lie close to the critical screening strengths for $3p$ and $2p$ states i.e. $\mu_D^c(3p) = 0.1127$ a.u. and $\mu_D^c(2p) = 0.2202$ a.u. Resonant screening strengths μ_r are slightly higher than the μ_D^c values for which $2p$ and $3p$ states enter into quasi bound regime. This means that when $\mu > \mu_D^c$, continuum state electron is trapped in $2p$ and $3p$ quasi bound states for comparatively longer time leading to large overlap with bound 1s wave function.

We have plotted, in Figure 5 and 6, the continuum wave functions for both the resonance state energies. For comparison purpose the radial wave functions corresponding to energies away from resonance is also plotted. It is clearly seen that there is strong enhancement in the amplitude of resonant state wave function in comparison to others in the atomic volume. This leads to large overlap matrix element leading to very high value of cross section. We have also indicated the phase difference between these states as insets in respective plot. The plots show a phase change of π between resonant and away from resonant states. The same feature is also observed in behaviour of phase shift as depicted in Figure 1 and 2. In Figure 7, we have plotted the $\sigma_{1s\to\epsilon p}$ for some near critical screening values. It is observed that when the difference $(\mu - \mu_r)$ increases, the resonance peak gets reduced in height as well as becomes comparatively broader. This is because with further increase in μ beyond critical value, the centrifugal barrier width decreases so that it becomes easier for the photo electron to escape from the quasi bound state via quantum tunneling. This phenomenon is reflected as broad resonance structures. These resonances are also observed in multi-electron systems which are subjected to Debye screening [27, 28].

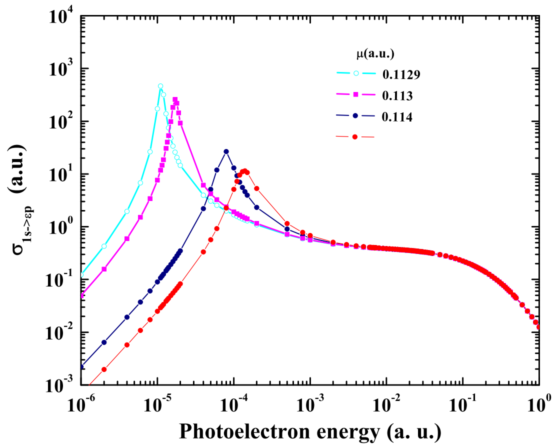

Figure 7. Behaviour of shape resonance peaks for near critical screening strengths.

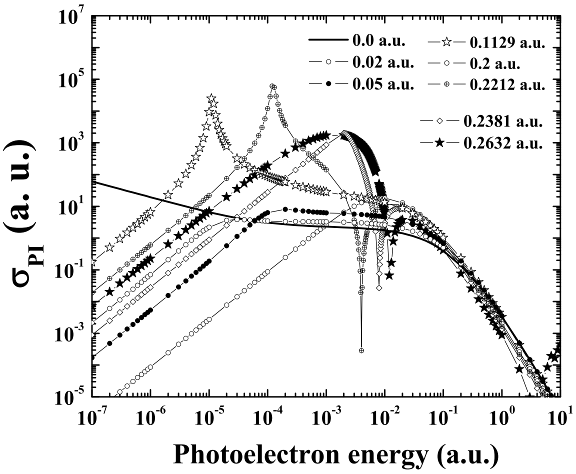

Figure 8. Variation of photoionization cross section from $2s$ state of Hydrogen atom with photoelectron energy.

Cooper minimum which corresponds to minimum in the photoionization cross section is another interesting feature arising due to Debye screening. Generally, the bound state having at least one node in its radial wave function exhibit this behaviour. In this work, we have observed Cooper minimum in the photoionization cross section from excited $2s$ state of hydrogen atom. The $\sigma_{2s\to\epsilon p}$ is plotted in Figure 8 which shows appearance of Cooper minimum for $\mu = 0.2212$ a.u. along with the shape resonance structure arising due to quasi bound $2p$ state. Essentially, the perturbation in the micro-field around the ion results in variation of phases and amplitudes of overlapping bound and free state wave functions. For certain plasma condition, the positive and negative components of the oscillatory bound and continuum states just cancel each other leading to zero in the dipole matrix element. We have noticed that as μ value is increased the position of Cooper minimum shifts towards higher photo electron energy. Cooper minimum in $\sigma_{2s\to\epsilon p}$ appears in the energy range $\epsilon \sim (4-12)\times 10^{-3}$ a.u. which is close to the value $\epsilon = (8-25)\times 10^{-3}$ Rydberg reported by Qi et al. [17].

4. Conclusion

Effect of plasma screening on ground and excited state photoionization cross section of hydrogenic system is investigated. In a weakly coupled plasma, the centrifugal barrier in the DH potential can support quasi bound states arising due to pressure ionization of bound levels. The transition from bound state to these quasi bound states gives rise to resonance structures in photoionization cross section. These resonances are termed as 'Shape resonance' as these are related to the shape of potential barrier. It is also observed that the appearance of shape resonances are related to the phase of the continuum waves. For particular plasma condition, screening introduces a phase shift of π radian in the continuum state wave functions. Around these screening values, we can observe shape resonance peaks in the photoionization curve. The changes in phase and amplitude of continuum wave also affect the cross section for transition from excited state. In case of hydrogen like ions we observe Cooper minimum in the $2s-\epsilon p$ cross section after the shape resonance peak. The Cooper minimum is absent in $\sigma(1s)$ and appears for states which have atleast one node in its radial wave function. These remarkable changes produced in the photoionization cross section may affect radiative and spectroscopic properties of plasma as a whole.

Competing Interests

The authors declare that they have no competing interests.

Authors' Contributions

Both the authors contributed equally and significantly in writing this article. Both the authors read and approved the final manuscript.

References

[1] F. Anthony, Starace, photoionization of atoms, *Research Papers in Physics and Astronomy*, 1996.

[2] J. J. Yeh and I. Lindau, Atomic subshell photoionization cross sections and asymmetry parameters: $1 \le Z \le 103$, *At. Data. & Nucl. Data. Tables.*, **32** (1985), 1–155.

[3] D. Salzman, *Atomic Physics in Hot Dense Plasma*, New York: Oxford; 1998.

[4] M. S. Murillo and J. C. Weisheit, Dense plasmas, screened interactions, and atomic ionization, *Phys. Rep.*, **302** (1998), 1–65.

[5] S. Atzeni and J. Meyer-ter-Vehn, *The Physics of Inertial Fusion: Beam Plasma Interaction, Hydrodynamics, Hot Dense Matter*, New York: Oxford University Press, 2004.

[6] J. A. Kunc and W. H. Soon, Maximum principal quantum numbers of the atomic hydrogen in the solar chromosphere and photosphere, *Astro. J.*, **396** (1992), 364–368.

[7] N. Kryukov and E. Oks, Ionization channel of continuum lowering in plasmas: effects of plasma screening, electric and magnetic fields, *J. Phys. B: At. Mol. Opt. Phys.*, **46** (2013), 245701-245701-10.

[8] M. W. C. Dharma-wardana, Level shifts, continuum lowering, and the mobility edge in dense plasmas, *Phys. Rev. A*, **45** (1992), 5883-5896.

[9] H. R. Griem, *Principles of Plasma Spectroscopy*, Cambridge: Cambridge University Press, 1997.

[10] John C. Stewart and Kedar D. Pyatt, Lowering of ionization potentials in plasma, *Astrophysical J.*, **144** (1966), 1203-1211.

[11] G. Chiu and A. Ng, Pressure ionization in dense plasmas, *Phys. Rev. E*, **59** (1999), 1024-1032.

[12] R. M. More, Pressure ionization, resonances, and the continuity of bound and free states, *Adv. At. Mol. Phys.*, **21** (1985), 305-356.

[13] M. Nantel, G. Ma and S. Gu et al., Pressure ionization and line merging in strongly coupled plasmas produced by 100-fs laser pulses, *Phys. Rev. Lett.*, **80** (1998), 4442-4445.

[14] G. B. Zimmerman and R. M. More, Pressure ionization in laser-fusion target simulation, *J. Quant. Spectrosc. Radiat. Transfer*, **23** (1980), 517-522.

[15] V. E. Fortov, V. Ya. Ternovo and M. V. Zhernokletov et al., Pressure-produced ionization of nonideal plasma in a megabar range of dynamic pressures, *J. Expt. Th. Phys.*, **97** (2003), 259–278.

[16] Y. Jung, Plasma screening effects on photoionizations in weakly coupled plasmas, *Phys. Plasma*, **5** (1998), 3781.

[17] Y. Y. Qi, J. G. Wang and R. K. Janev, Dynamics of photoionization of hydrogen like ions in Debye plasmas, *Phy. Rev. A*, **80** (2009), 063404.

[18] C. Y. Lin and Y. K. Ho, Effects of screened coulomb abd exponential cosine-screened Coulomb potentials on photoionization of H and He^+, *Eur. Phys. J. D*, **57** (2010), 21.

[19] T. Utsumi and J. Koga, Accurate numerical method for the solutions of the Schrödinger equation and the radial integrals based on the CIP method, *Comp. Phy. Comm.*, **148** (2002), 267-280.

[20] S. T. Manson, *Topics in Appl. Phys.* **26** (1978), 135.

[21] A. Burgess and M. J. Seaton, A general formula for the calculation of atomic photo-ionization cross sections, *Monthly Notices of the Royal Astronomical Society*, **120** (1960), 121-151.

[22] B. H. bransden and C. J. Joachain, *Physics of Atoms and Molecules*, Singapore: Pearson Education, 2004.

[23] http://physics.nist.gov/cgi-bin/ASD/energy1.pl

[24] B. Saha, P. K. Mukherjee and G. H. F. Diercksen, Energy levels and structural properties of compressed hydrogen atom under Debye screening, *Astronomy and Astrophysics*, **396** (2002), 337-344 .

[25] H. R. Sadeghpour, J. L. Bohn and M. J. Cavagnero et al. Collisions near threshold in atomic and molecular physics, *J. Phys. B: At. Mol. Opt. Phys.*, **33** (2000), R93-R140.

[26] M. Bylicki, A. Stachow, J. Karwowski and P. K. Mukherjee, The resonance levels of the Yukawa potential, *Chem. Phys.*, **331** (2007), 346-350.

[27] M. Das, Effect of strongly coupled plasma on photoionization cross section, *Phys. Plasmas*, **21** (2014), 012709.

[28] C. Y. Lin and Y. K. Ho, Influence of Debye plasma on photoionization of Li-like ions: Emergence of Cooper minimum, *Phys. Rev. A*, **81** (2010), 033405.